Aging Cell (2013) **12**, pp398–409 Doi: 10.1111/acel.12063

WormFarm: a quantitative control and measurement device toward automated *Caenorhabditis elegans* aging analysis

Bo Xian,[1,3]* Jie Shen,[2]* Weiyang Chen,[1]* Na Sun,[1,3] Nan Qiao,[1,3] Dongqing Jiang,[2] Tao Yu,[1] Yongfan Men,[2] Zhijun Han,[1] Yuhong Pang,[2] Matt Kaeberlein,[4] Yanyi Huang[2] and Jing-Dong J. Han[1]

[1]CAS Key Laboratory for Computational Biology, CAS-Max Planck Partner Institute for Computational Biology, Shanghai Institutes for Biological Sciences, Chinese Academy of Sciences, 320 Yueyang Road, Shanghai 200031, China
[2]College of Engineering and Biodynamic Optical Imaging Center (BIOPIC), Peking University, Beijing 100871, China
[3]Center for Molecular Systems Biology, Institute of Genetics and Developmental Biology, Chinese Academy of Sciences, Lincui East Road, Beijing 100101, China
[4]Department of Pathology, University of Washington, Seattle, WA 98195, USA

Summary

***Caenorhabditis elegans* is a leading model organism for studying the basic mechanisms of aging. Progress has been limited, however, by the lack of an automated system for quantitative analysis of longevity and mean lifespan. To address this barrier, we developed 'WormFarm', an integrated microfluidic device for culturing nematodes. Cohorts of 30–50 animals are maintained throughout their lifespan in each of eight separate chambers on a single WormFarm polydimethylsiloxane chip. Design features allow for automated removal of progeny and efficient control of environmental conditions. In addition, we have developed computational algorithms for automated analysis of video footage to quantitate survival and other phenotypes, such as body size and motility. As proof-of-principle, we show here that WormFarm successfully recapitulates survival data obtained from a standard plate-based assay for both RNAi-mediated and dietary-induced changes in lifespan. Further, using a fluorescent reporter in conjunction with WormFarm, we report an age-associated decrease in fluorescent intensity of GFP in transgenic worms expressing GFP tagged with a mitochondrial import signal under the control of the *myo-3* promoter. This marker may therefore serve as a useful biomarker of biological age and aging rate.**

Key words: aging; automatic; *C. elegans*; microfluidics; phenotype; quantitative analysis.

Correspondence
Jing-Dong J. Han, CAS Key Laboratory for Computational Biology, CAS-Max Planck Partner Institute for Computational Biology, Shanghai Institutes for Biological Sciences, Chinese Academy of Sciences, 320 Yueyang Road, Shanghai, 200031, China. Tel.: 86 21 54920458; fax: 86 21 54920504; e-mail: jdhan@picb.ac.cn
or
Yanyi Huang, College of Engineering, and Biodynamic Optical Imaging Center (BIOPIC), Peking University, Beijing, 100871, China. Tel.: 86 10 62758323; fax: 86 10 62758323; e-mail: yanyi@pku.edu.cn

*These authors contributed equally to this work.

Accepted for publication *12 February 2013*

Introduction

The nematode *Caenorhabditis elegans* has been a primary model organism for studying basic mechanisms of aging. Powerful *C. elegans* genetics have enabled discovery of hundreds of lifespan extending mutations and delineated novel longevity pathways. Moreover, phenotypic assays have been developed that allow quantitative assessment of mean lifespan (Huang *et al.*, 2004; Gerstbrein *et al.*, 2005; Leiser *et al.*, 2011). Importantly, several of the aging-related factors uncovered from studies in *C. elegans*, such as the insulin/IGF-1 signaling (IIS) pathway and the target of rapamycin (TOR) kinase, are now known to similarly modulate longevity and aging in mammals (Kenyon, 2010).

As a widely used model system for aging-related studies, maximal lifespan and mean lifespan analyses in *C. elegans* are essential experiments in many laboratories. However, the standard assays are tedious, time-consuming, and susceptible to human bias and technical variations. For example, to measure lifespan, researchers typically maintain animals on Nematode Growth Medium (NGM) agar plates with a lawn of *Escherichia coli* OP50 as the food source (Brenner, 1974; Sutphin & Kaeberlein, 2009). Adult animals must be transferred to fresh plates every few days to prevent depletion of the food source or contamination with progeny. The amount of manual labor required to perform lifespan analysis in *C. elegans* can be reduced somewhat using the drug 2′-deoxy-5-fluorouridine (Floxuridine, FUdR) to prevent hatching of eggs (Mitchell *et al.*, 1979; Gandhi *et al.*, 1980); however, animals must still be periodically transferred to fresh NGM plates to avoid contamination and maintain stable RNAi efficacy and are manually assessed for viability every 2–4 days.

In addition to the large amount of effort required to perform longevity studies in *C. elegans*, a variety of environmental factors limit the quantitative resolution and reproducibility of these assays. For example, contamination of the NGM agar with bacteria and/or fungi, variation in temperature and moisture, and loss of animals due to foraging are all likely to contribute to variations between experiments within the same laboratory and among different laboratories. Addition of FUdR may also influence longevity under some conditions, such as its reported effect of enhancing the lifespan of *tub-1* mutants (Aitlhadj & Sturzenbaum, 2010), masking lifespan extension caused by *ash-2(RNAi)* (Greer *et al.*, 2010), and affecting the identification of metabolic responses to *daf-2* status (Davies *et al.*, 2012).

Lifespan assays can also be performed on solid NGM overlaid with a liquid layer (Bishop & Guarente, 2007). However, these types of protocols are less commonly employed, because several potential problems have thus far limited the utility and generality of liquid-based longevity protocols. These include the difficulty in separating adult hermaphrodites from their progeny (without FUdR) and the need to frequently transfer the worms to fresh medium over the course of the lifespan. Relative to the number of studies performed

© 2013 John Wiley & Sons Ltd and the Anatomical Society

on solid media, there are far fewer reports of quantitative lifespan assays performed in liquid culture, and these have generally been low throughput (Hulme *et al.*, 2010).

An automated method to quantitatively measure survival and age-related phenotypes would represent a major breakthrough in methodology and benefit the field substantially. Microfluidics-based systems for culturing nematodes offer an attractive approach toward developing such a system. For example, Hulme *et al.* have recently proposed a microfluidic method to make lifelong observations of a few animals (Hulme *et al.*, 2010). To date, however, no practical microfluidic device for monitoring and collecting lifelong age-related data on a large population of animals has been described. Here, we present such a system. WormFarm is an integrated microfluidic platform to maintain groups of nematodes during adulthood, along with a set of algorithms to quantitate survival and age-related phenotypes from images and videos. As proof-of-principle, we performed survival analysis of wild-type (N2) animals subjected to three RNAi knockdowns and glucose treatment previously reported to influence longevity. We also carried out real-time fluorescence imaging of intestinal auto-fluorescence and muscle-expressed mitochondria-targeted GFP (*Pmyo-3::mito::GFP*) in animals as they aged. This novel approach allowed us to identify a previously undetected reduction in *Pmyo-3::mito::GFP* fluorescence with age. This trend was observed in all RNAi and control strains and scaled to lifespan, suggesting that this marker may serve as a useful biomarker of biological age or rate of aging.

Results

The design of WormFarm platform

The WormFarm platform is composed of 3 modules: food/medium loading module, WormFarm chip, and image acquisition module. The food suspension (*E. coli* OP50) is stored inside the 15-ml conical bottom culture tubes with tubing connected to the microfluidic chip. Compressed air is used to drive the food into the culture chambers on-chip (Fig. 1).

The WormFarm chip is a multilayer polydimethylsiloxane (PDMS) microfluidic device with monolithic integrated controllable valves (Fig. 1). The eight chambers (3×10 mm^2 each) per chip are completely separated from each other to prevent cross-contamination and are optimized to culture ~ 40 animals per chamber (Fig. 1). The upper boundaries of the chambers are arc-shaped to prevent liquid and small larvae from being trapped in corners. The typical thickness of an N2 adult worm is ~ 90 μm; thus, the height of the chamber is 100 μm to allow the animals to move freely. At the downstream boundary of the chamber, there is a channel-comb, composed of a row of small channels, each of which is 20 μm wide and 10 μm high. These channels function like a sieve, preventing passage of adult animals but filtering L1 or L2 larvae from the chamber. To prevent blocking of the sieve channels by adult animals, extra sieve channels were also placed on the sides of the chamber. Bypass channels are present in each culture chamber to remove air bubbles when loading samples and food/medium. All channels are controlled by monolithic pneumatic valves (Unger *et al.*, 2000; Thorsen *et al.*, 2002) (Fig. 1). Waste is discharged from the outlets of the chambers via tubing connections. These exits may also be used to collect the larvae if desired, for example, to examine phenotypic changes in progeny as a function of parents' age. If recovery of adults is desired, the chambers can be reversely flushed with culture medium to remove the animals from inlets. PDMS is intrinsically transparent, allowing visualization of the animals inside the culture chambers by microscopy using standard equipment.

Loading and operating the device

Each PDMS chamber is designed to be loaded with approximately 40 adult nematodes (Fig. S1, Video S1, S2). Prior to loading the

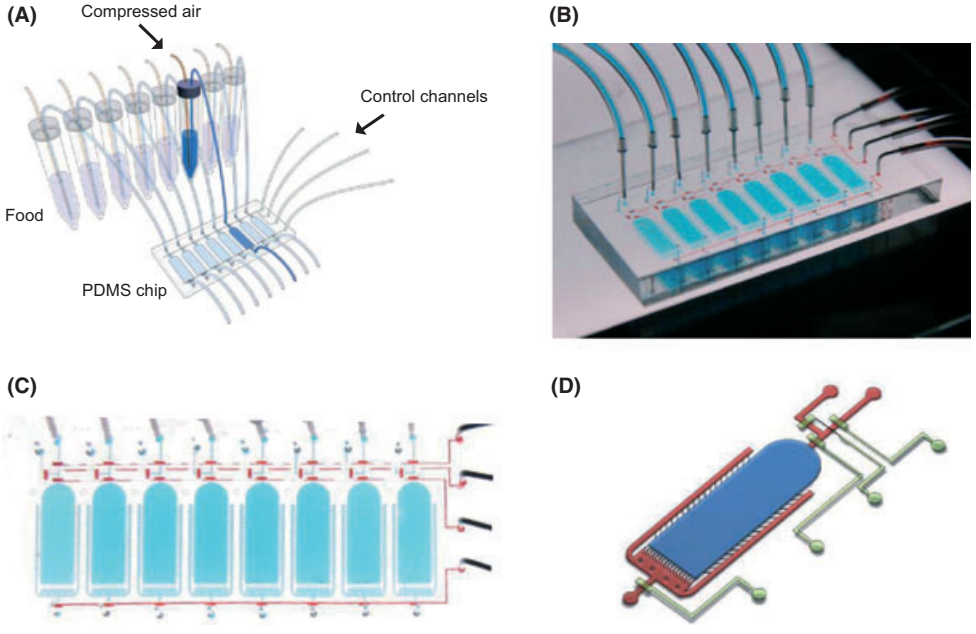

Fig. 1 Design of the WormFarm system. (a) Schematic of the WormFarm platform. (B) A photograph of the WormFarm chip. A 25×55 mm^2 chip is mounted at the center of a 70×100 mm^2 glass slide. (C) Each chip contains eight separated chambers, which can be controlled by the pneumatic valves simultaneously. (D) 3D schematic of a single WormFarm chamber, with narrow channels at side and bottom edge to filter out the worm progeny by size.

© 2013 John Wiley & Sons Ltd and the Anatomical Society

animals, each chamber is incubated with 0.2% Pluronic solution [0.2% w/v cell culture grade Pluronic F127 (Sigma, St. Louis, MO, USA)] for 30 min followed by rinsing with S-Medium. Pluronic solution is a kind of surface-activating agent, which prevents free bacteria from depositing on the surface of the PDMS. Following the rinse, 200 μL of a suspension containing synchronized young adult animals in S-Medium (~ 200 nematodes mL^{-1}) is then loaded in each chamber and the valves are closed. Food supply tubes are then connected to provide a flow of bacterial food to each chamber. Here, we used the bacterial concentrations of 10^9 cell mL^{-1} in S-Medium for liquid culture (Bishop & Guarente, 2007) to ensure sufficient food for the worms. The valves for worm loading are closed after loading. Flow rates and number of animals are visually optimized to the minimal flow that can disperse the worms at a comfortable level and wash out the progenies. As a result of such testing, the period of the flow cycle of the food/medium supply is set to 2.5 min, and the flow/stop ratio of each cycle was set to be 0.25 (0.5 min influx with 2 min in between) through the control of the valves. Under these conditions, all progeny are washed out of the chambers through the outlets as L1 or L2 larvae (Video S3). This eliminates the need for adding FUdR to the medium.

Validation of WormFarm for nematode culture

A critical first test of WormFarm is to verify that the health of animals maintained in the microfluidic chamber is similar to animals aged under conventional agar-plate-based conditions. We therefore performed parallel studies of animals maintained either in WormFarm or on NGM plates from adult day 2 to adult day 8 and quantified the size of worms under both conditions. As the densities and environments of worms are quite different in those two conditions, the worms in chips were generally smaller than those on plates. However, the inter-strain differences largely followed the same trend, and the worms' average body size increased from day 2 to day 5 in most of the strains under both conditions (Fig. S2). These indicate that the worms in WormFarm grew as well as those on plates.

The automation of progeny separation, continuous food supply, and waste control are obvious advantages of WormFarm over the conventional approaches. In this study, we typically carried out experiments with 2–4 WormFarm chips simultaneously. Using a 2-chip experiment as an example, once the chambers are loaded, lifespan is determined for ~ 640 animals without requiring additional manual intervention. For comparison, the same experiment performed using the standard plate-based assay would require manual transfers of ~ 640 animals at least 3–5 times and manual determination of viability for each animal by prodding every 2–3 days. Thus, WormFarm provides a much simpler, less invasive, and more efficient way to perform these types of experiments with the added advantage of providing dynamic control of the culture conditions.

Validation of WormFarm for RNAi studies

RNAi has proven to be a particularly powerful technique to probe genetic regulation of aging in *C. elegans*. To determine whether WormFarm can be used to quantitate lifespan in conjunction with RNAi knockdown, N2 animals were aged in WormFarm and fed with HT115 bacteria containing either an empty-vector control plasmid or sequence-confirmed RNAi plasmids targeting *sptf-3*, *Y82E9BR.3*, or *age-1* from a genome-wide RNAi library, the Ahringer library (Fraser *et al.*, 2000; Timmons *et al.*, 2001). Survival was determined by video microscopy of each WormFarm chamber. RNAi knockdown of *sptf-3* is reported to result in shorter lifespan (Xue *et al.*, 2007), while knockdown of an ATP synthesis gene such as *Y82E9BR.3,* reduces body size and extends lifespan (Lee *et al.*, 2003). In both cases, the lifespans obtained from animals aged in WormFarm showed the expected trends and matched the survival of animals aged on NGM plates (Fig. 2, Fig. S3, Table 1). In the case of *Y82E9BR.3(RNAi)*, the body size reduction and the developmental delay were clearly observed in animals cultured in WormFarm, while *sptf-3(RNAi)* resulted in a shorter lifespan than the control group, as previously described (Xue *et al.*, 2007) (Fig. 2, Video S3).

The IIS pathway is the best-characterized longevity pathway in *C. elegans*. Reduced signaling through this pathway leads to the activation of FOXO-family transcription factor DAF-16 (Lin *et al.*, 1997; Ogg *et al.*, 1997) and results in robust lifespan extension. Reduction-of-function mutations or RNAi knockdown of several components of this pathway, including the genes encoding the insulin-like receptor *daf-2* or the PI3-kinase *age-1*, has been reported by many laboratories to enhance longevity (Johnson, 1990; Morris *et al.*, 1996; Kenyon, 2005). As further validation of WormFarm, we examined the effect of RNAi knockdown of *age-1* on animals maintained in WormFarm. As expected, lifespan was significantly extended relative to control animals.

In all of these experiments, RNAi knockdown was carried out by simply replacing the OP50 suspension with the appropriate RNAi bacterial strain grown under inducing conditions. Even though the repeats of RNAi lifespan assays were derived from independent chips, both the survival rates on each day (Fig. 2, Fig. S3c) and the overall mean lifespan differences (Table S1) showed good repeatability of WormFarm.

Viability of individual animals in WormFarm is determined from videos that are acquired daily using an algorithm we developed (see below). This is a substantial improvement in efficiency compared with the manual determination of viability by gently tapping each animal on the head to tell whether it is alive or dead. WormFarm allows for automatic collection and in-line analysis of the quantitative imaging data, which is acquired as frequently as required.

Effect of glucose supplementation on lifespan using WormFarm

In addition to the reduced time, effort, and resources required to perform aging-related analyses using WormFarm, the ease with which the effects of different medium compositions can be examined is a major advantage of this system. Changes in medium compositions could involve dietary interventions, such as dietary restriction, or pharmacological interventions for drug screening and/or toxicology studies.

© 2013 John Wiley & Sons Ltd and the Anatomical Society

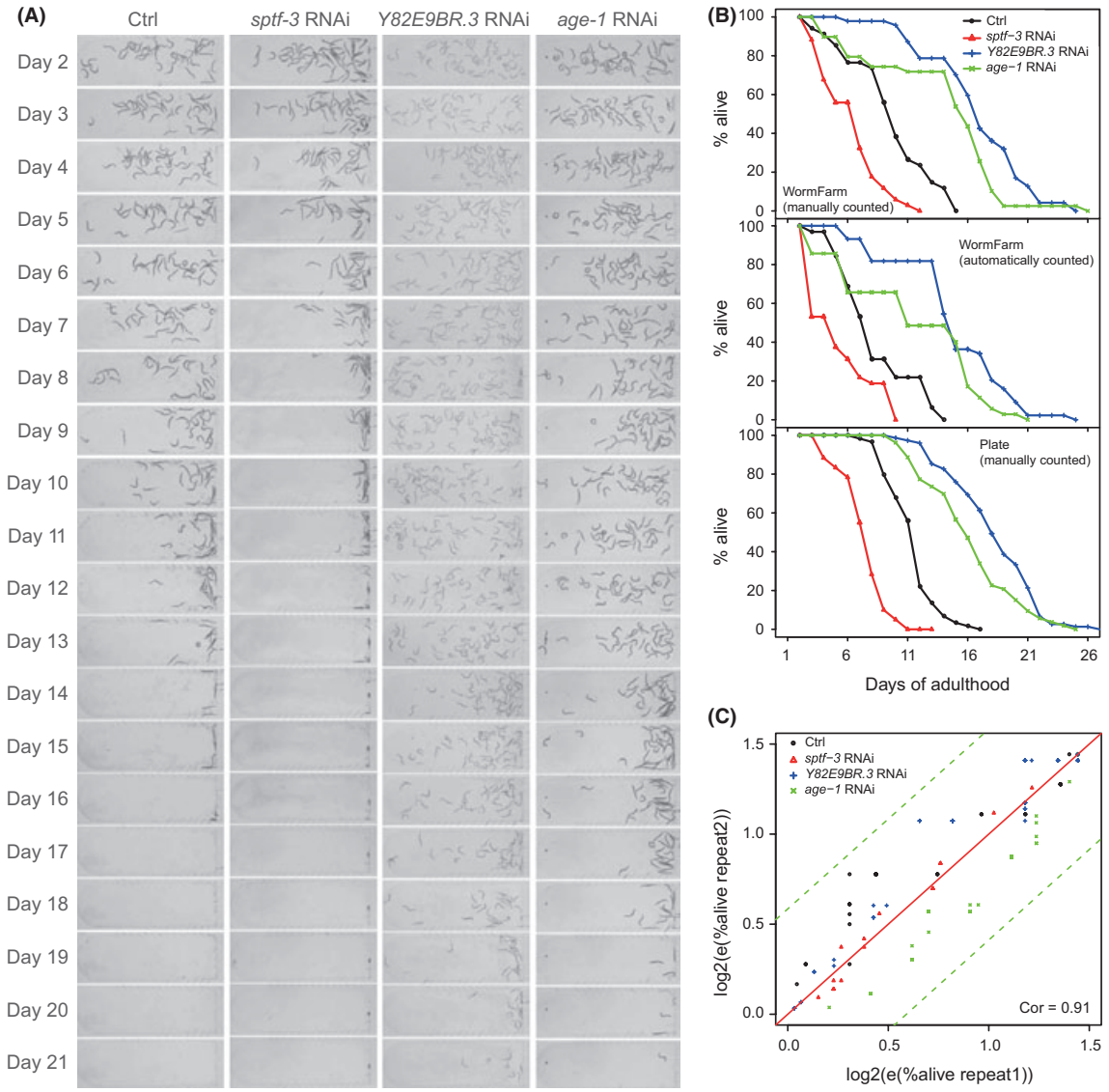

Fig. 2 Lifespan assays for worms fed RNAi bacteria in WormFarm. (A) Photographs of worms living in WormFarm PDMS chambers under different RNAi conditions. (B) Survival rate curves of worms in PDMS chambers upon different RNAi conditions when live worms were determined manually by watching movies (upper panel) or by computational program analyzing the movies (middle panel), and the survival rate curves of worms under different RNAi treatments on NGM plates when live worms were determined by conventional method (lower panel). The day of egg-laying was defined as day 0 in all the experiments in this study. Lifespan of adulthood were obtained at 25 °C. (C) Scatter plots showing the repeatability of each group of two biological replicates in different chambers on different chips. Survival rates of two different repeats are plotted against each other across the worm adult lifespan. The *x*- and *y*-axes indicate the survival rates of repeat 1 and repeat 2 on the indicated day of adult life, respectively. Pearson correlation coefficient ('Cor') between the repeats for all four groups is shown at the bottom of the panel. Raw data are available in Table S4 (Supporting Information).

One dietary intervention that has been reported to shorten *C. elegans* lifespan is addition of glucose to the diet (Schulz *et al.*, 2007; Lee *et al.*, 2009; Schlotterer *et al.*, 2009). Consistent with this, we observed that supplementation with either 2 or 4% glucose shortened the lifespan of animals aged in WormFarm or on NGM agar plates (Fig. 3, Fig. S4a). These experiments demonstrate that WormFarm is able to detect subtle effects on longevity, such as the ~ 15% average lifespan reductions induced by 2 or 4% glucose compared with control (Table 2). Furthermore, these experiments again demonstrate good repeatability of the survival rates of worms on each day (Fig. 3, Fig. S4c) of the WormFarm system, which is similar to that obtained by routine on-plate experiments (Fig. S4b), and also good repeatability of the overall mean lifespan differences (Table S2) among independent devices. Overall, subtle environmental differences, such as the concentration and the form of food, and differences in humidity and temperature can be precisely controlled in WormFarm, resulting in very good repeatability (Fig. 2, 3, Fig. S3c, S4c, Table S1 and S2).

Quantitative phenotypic analysis in WormFarm assisted by automatic imaging analysis

The tremendous amount of data (~ 100 GB of images and video per experiment), automatically collected by WormFarm, provides both

© 2013 John Wiley & Sons Ltd and the Anatomical Society

Table 1 Significance of deviation of a survival rate curve from the control curve in RNAi experiments

Group	RNAi	Mean lifespan (day)	Max lifespan (day)	Standard deviation	Mean lifespan change (%)	*n*	*P*-value
WormFarm manually counted	ctrl	8.676470588	14	3.435294423		34	
	sptf-3	5.382352941	11	2.474288461	−37.97	34	6.39E-06
	age1	13	25	5.472418882	49.83	39	1.84E-07
	Y82E9BR.3	15.93617021	24	4.088181563	83.67	47	9.66E-15
WormFarm automatically counted	ctrl	7.34375	13	3.064988291		32	
	sptf-3	4.34375	9	2.719219231	−40.85	32	0.000687
	age1	10.6	20	5.595165981	44.34	35	0.000127
	Y82E9BR.3	13.93181818	24	4.505282312	89.71	44	1.33E-12
NGM plate	ctrl	10.45762712	16	1.985482083		59	
	sptf-3	6.483333333	10	1.836463686	−38.00	60	< 2.2E-16
	age1	15.22641509	24	3.739814421	45.60	53	5.7E-14
	Y82E9BR.3	17.24	26	3.552083515	64.86	75	< 2.2E-16

an opportunity and a challenge for quantitative analysis. To maximize the information obtained from each experiment, we developed computational image analysis algorithms (Experimental procedures and Note S1) to automatically analyze the video footage and quantitate survival rate (live or dead worms) and other phenotypes including worm size, length, width, shape, and content density. (Fig. 4, Video S4, 5). These algorithms generated similar survival curves to those obtained by manual analysis and correctly recapitulated the observed differences in lifespan for all of the experiments (Table S1, S2). In addition, they provide quantitative analysis of the body size and motility parameters with age in real time. Using these algorithms, we found that the long-lived *age-1(RNAi)* and *Y82E9BR.3(RNAi)* animals were significantly thinner (Student's *t*-test $P = 2.2e\text{-}16$ and 3.39e-12, respectively. Fig. 4) and more active than the control group (Fig. 4, $P = 3.43e\text{-}9$ and 1.75e-6, respectively). In contrast, the short-lived *sptf-3(RNAi)* animals had larger body width (Fig. 4, $P = 4.83e\text{-}2$). The motility of *sptf-3(RNAi)* animals was significantly less than the other three groups ($P = 3.35e\text{-}5$, 2.2e-16, and 1.05E-12 vs. control, *age-1,* and *Y82E9BR.3*, respectively, Fig. 4 and Table S3). In fact, if the anatomical features of the single worms in each picture were classified using principal component analysis (PCA), the first and third principal (PC1 and PC3) components jointly separated the *Y82E9BR.3(RNAi)* strain from the other three strains, and the young and old worm in each strain were distributed diagonally between PC1 and PC3 (Fig. 4). The major contributing features to PC1 are size (0.44) and mean gray density (−0.43), while shape and gray density distribution contribute the most to PC3 (−0.67 and −0.52, respectively), suggesting these features are most associated with age.

These phenotypic data demonstrate yet another significant advantage of WormFarm: multiple aging-related phenotypes can be simultaneously, automatically, and quantitatively analyzed.

Fluorescence-based phenotypic analysis in WormFarm assisted by automatic imaging analysis

In addition to light microscopy, the WormFarm PDMS chambers are also compatible with fluorescence microscopy, and a variety of transgenic fluorescent protein reporters have been constructed for use in *C. elegans*. Of particular interest with respect to age-related changes are markers of mitochondrial biogenesis and function. Enhanced mitochondrial biogenesis is associated with improved mean lifespan in mammals, and mitochondrial gene expression has been shown to decrease with age in many different organisms and tissues (McCarroll *et al.*, 2004; Zahn *et al.*, 2007). For example, we have previously reported that a gene expression module enriched for genes encoding mitochondrial enzymes showed a linear decline with age in adult *Drosophila melanogaster* (Xue *et al.*, 2007).

To examine whether we can detect fluorescence changes *in vivo* with age in live *C. elegans*, we used WormFarm to examine the age-dependent changes in animals expressing a mitochondrial-targeted GFP in muscle cells (*Pmyo-3::mito::GFP*). Consistent with age-dependent oxidative phosphorylation gene expression decline, we observed a continuous decline in fluorescent intensity of GFP with age in worms grown in WormFarm. This decline was very rapid during early adulthood (day 2–7) and slowed down afterward (Fig. 4). RNAi knockdown of *sptf-3*, which shortened lifespan, accelerated the age-dependent decline in GFP fluorescence intensity, while RNAi knockdown of *Y82E9BR.3*, which increased lifespan, delayed the decline (Fig. 4, Fig. S5a). These data suggest that fluorescence intensity of this GFP reporter may serve as a biomarker of biological age and that the rate of the decline may serve as an estimate of aging rate.

Other well-known age-related markers, such as increased intestinal autofluorescence of *C. elegans* during aging (Klass, 1977; Davis *et al.*, 1982; Joeng *et al.*, 2004; Pincus & Slack, 2010), can also be precisely and easily quantified with WormFarm (Fig. 4).

Oxidative stress tolerance assay in WormFarm

In addition to analyzing phenotypes throughout the lifespan of worms, other aging-related parameters can also be quantitatively measured with WormFarm. For example, it is often useful to measure resistance to different forms of stress in addition to lifespan when studying factors that influence longevity. Oxidative stress in particular is linked to aging and lifespan (Finkel & Holbrook, 2000). Using WormFarm, we were able to quantitate increased tolerance to the superoxide generating compound paraquat upon RNAi knockdown of *daf-2*, as well as the greater sensitivity of animals subjected to *daf-16* RNAi (Fig. S6), with differences in survival similar to those

© 2013 John Wiley & Sons Ltd and the Anatomical Society

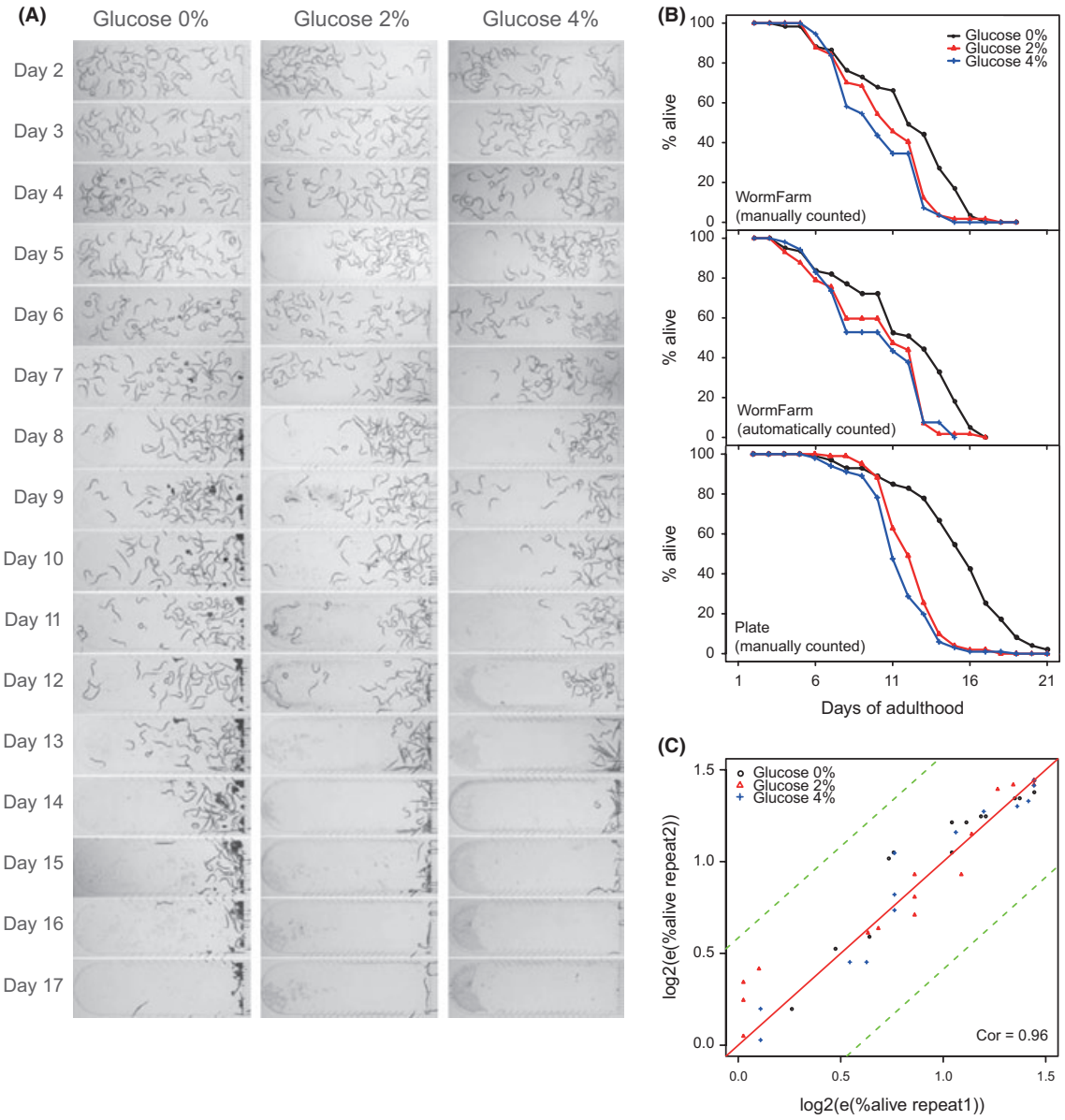

Fig. 3 Lifespan assays for worms in glucose medium. (A) Photographs of worms living in WormFarm PDMS chambers. (B) Survival rate curves of worms in PDMS chambers under different concentrations of glucose when live worms were determined manually by watching movies (upper panel) or by computational program analyzing the movies (middle panel), and the survival rate curves of worms under different concentrations of glucose on NGM plates when live worms were determined by conventional method (lower panel). Lifespan of adulthood was obtained at 25 °C. Live bacteria were fed to the worms according to a previous study (Lee *et al.*, 2009). (C) Scatter plots showing the repeatability of each group of two biological replicates in different chambers on different chips. Survival rates of two different repeats against each other across the worm adult lifespan. The *x*- and *y*-axis indicate the survival rates of repeat 1 and repeat 2 on the indicated day of adult life, respectively. Pearson correlation coefficient ('Cor') between the repeats for all three groups is shown at the bottom of the panel. Raw data are available in Table S4 (Supporting Information).

previously reported (Martin *et al.*, 1996; Finkel & Holbrook, 2000). Like many chemicals, paraquat is an expensive reagent. The drastically reduced volumes required for these types of assays in WormFarm reduces the amount of drug required to ~ 1/100 of what is normally consumed in a multiwell plate assay system.

Discussion

As an automated system based on liquid culture in a PDMS chip, WormFarm is a breakthrough for aging-related and survival-based analyses. WormFarm provides a simple, scalable platform for performing high-throughput survival and quantitative fluorescence assays in *C. elegans* at a cost that is substantially reduced relative to the current state-of-the art methods used in the field.

Although there are small differences in the survival data obtained from WormFarm relative to the standard plate-based method, in every case, the relative effects of different genetic and environmental interventions are quite similar. The differences likely arise from environmental factors, such as liquid versus solid medium culture conditions, worm densities. There are also differences between computer-assisted quantitation and manual visual quantitation that might be mainly due to the different standards used in

© 2013 John Wiley & Sons Ltd and the Anatomical Society

Table 2 Significance of deviation of a survival rate curve for glucose diet from the control curve

Group	Growth condition (%)	Mean lifespan (day)	Max lifespan (day)	Standard deviation	Mean lifespan change (%)	*n*	*P*-value
WormFarm	Ctrl	10.94915254	16	3.490991998		59	
manually	Glucose 2	9.719298246	17	2.876967563	−11.23	57	0.004148
counted	Glucose 4	9.145454545	14	2.655659099	−16.47	55	8.99E-05
WormFarm	Ctrl	10.78688525	16	3.834556707		61	
automatically	Glucose 2	9.175438596	16	3.412805753	−14.94	57	0.000912
counted	Glucose 4	9.037735849	14	3.198330479	−16.22	53	0.000436
NGM plate	Ctrl	14.36363636	21	3.456595427		99	
	Glucose 2	11.3627451	17	1.855093153	−20.89	102	< 2.2E-16
	Glucose 4	10.58415842	18	2.164566131	−26.31	101	< 2.2E-16

judging viability of the worms. To achieve automation, the computer program has to use certain thresholds, whereas human eyes and judgment are not subject to the same limitation. However, in terms of counting the relative survival and lifespan differences, the computer algorithm performs as good as manual counting (Fig. S7).

For all of the age-related features except survival, we only used single worms (unclustered worms) in each chamber to ensure the accuracy of the quantitative phenotypes. As analyzing worm clusters is apparently a very complex issue for imaging analysis, even the most recent state-of-art algorithm (Wahlby *et al.*, 2012) cannot practically solve this issue, at least not for images generated from our WormFarm chip. Our worm-counting program can at least partially solve this problem, in that using our algorithm, counting clustered worms consistently improved the accuracy of survival rate calculation than without counting clustered worms (Fig. S7).

Microfluidic devices to automate lifespan assays in yeast have been reported recently (Lee *et al.*, 2012; Xie *et al.*, 2012). Such a device for *C. elegans* has been lacking prior to WormFarm. Pincus *et al.* have developed a practical minimally invasive individual-nematode culture system (MIINCS) (Pincus *et al.*, 2011). Our WormFarm differs from this system in several ways, including the following: (i) in MIINCS, one single egg at the prehatch 'pretzel' stage and a bacterial food source are deposited atop PEG-1000-methacrylate hydrogel pads, whereas WormFarm cultures up to 40 worms for a single chamber in the liquid providing higher throughput; (ii) to prevent progeny contamination, only a sterile strain can be used in MIINCS, whereas WormFarm is suitable for studies of reproductively competent strains without the need for FUdR; (iii) food is never changed in MIINCS, while food (or any other component of the culture medium) in WormFarm can be changed automatically and immediately at any point in the experiment; (iv) culturing the worms on the surface of the plate causes the worms to shrink over time in MIINCS, which does not happen in WormFarm; and (v) MIINCS has only been analyzed by a semi-automated software to quantitate various morphological and image-based features, whereas WormFarm uses a fully automated software to do so.

To further increase the throughput of WormFarm, intelligent sample movement and image acquisition are needed. Possible solutions include translation of the sample stage coordinated with auto-focusing and auto-triggering of camera and light source. Such automation improvements will not only relieve the burden from the researchers, realize even larger-scale experimental design, and save experimental time, but also improve the quality of images, and the precision of data analysis.

In summary, WormFarm is a powerful new resource for aging-related studies in *C. elegans*. For the first time, it is possible to perform fully automated lifespan assays and to obtain quantitative measures of phenotypes such as body size and motility as a function of age without requiring extensive manual manipulation. In addition to reduced manual labor, WormFarm provides many advantages over traditional methods, including (i) alleviating contamination by progeny without use of drugs that inhibit reproduction; (ii) providing improved environmental control; (iii) removing the potential for unintentional human bias by automated acquisition and analysis of images and movies; and (iv) dramatically reducing costs associated with consumption of reagents and chemicals. In this report, we have demonstrated that WormFarm successfully reproduces the expected effects of RNAi knockdown for factors that either shorten or increase lifespan. Further, we have shown that WormFarm can also be used to quantitate changes in the expression of a fluorescence-based reporter during aging and, in the process, discovered a previously unknown inverse relationship between *Pmyo-3::mito::GFP* intensity and age. Indeed, the mito-GFP used in this study appears to provide a useful biomarker of biological age, at least among the interventions tested here.

Experimental procedures

Fabrication of the WormFarm chip

Microfluidic chips were fabricated from polydimethylsiloxane (PDMS) (RTV 615 kit, GE Advanced Materials, Wilton, CT, USA) through multilayer soft lithography (Unger *et al.*, 2000; Thorsen *et al.*, 2002; Wang *et al.*, 2009). The master molds of fluid and control layers were made by photolithography. The silicon wafers were treated with hexamethyldisilazane (Alfa Aesar, Ward Hill, MA, USA) vapor for 3 min at room temperature (25 °C) before coating the photoresist. The hybrid master mold of the fluid layer was fabricated through a multistep photolithography to form the molds with different thickness. The large chambers for worm culture were made of 100-μm-thick negative photoresist (SU-8 2050,

© 2013 John Wiley & Sons Ltd and the Anatomical Society

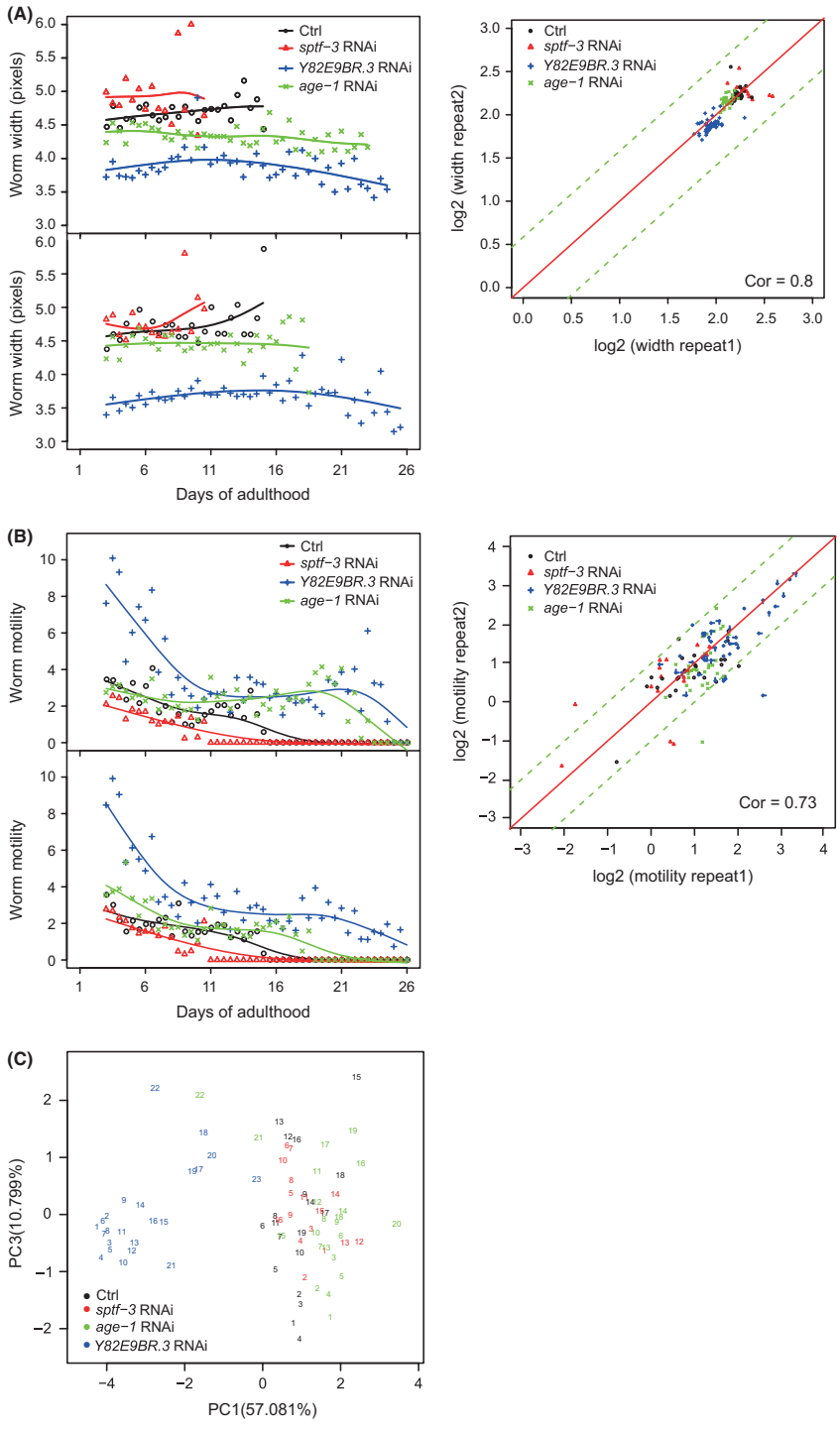

Fig. 4a Aging-related phenotypes quantified by WormFarm. (A, B) The widths and motilities of worms in WormFarm upon RNAi of aging-related genes. The left upper and lower panels display the results from two repeats. Movies taken on each day (Video S4, S5) were analyzed and quantified by our imaging analysis program. The right diagrams show the good repeatability of each group of 2 repeats. Pearson correlation coefficients ('Cor') between the repeats for all four groups are shown at the bottom of the panels. (C) Principal component analysis of various anatomical features of the worm. The worms are arranged according to the first and third principal components of worms' features. These features include shape, area, width, length, average gray value, variance of gray values, and the ratio of pixels brighter than defined threshold. PCA was performed on the average of each feature of all single worms for each age and each RNAi strain. Different RNAi strains are marked by different font colors of the numbers that indicate the age (days) of the worms. (D) *Pmyo-3::mito::GFP* fluorescent intensity over age. Left panels are the fluorescence images on the indicated days of adulthood of the indicated RNAi strains. Right panels show the quantified intensities in the body wall muscles per day per chamber plotted against age. Raw data are available in Table S5 and S6 (Supporting Information). (E) Photographs and quantitation of intestinal auto-fluorescence intensity of N2 worms over age.

© 2013 John Wiley & Sons Ltd and the Anatomical Society

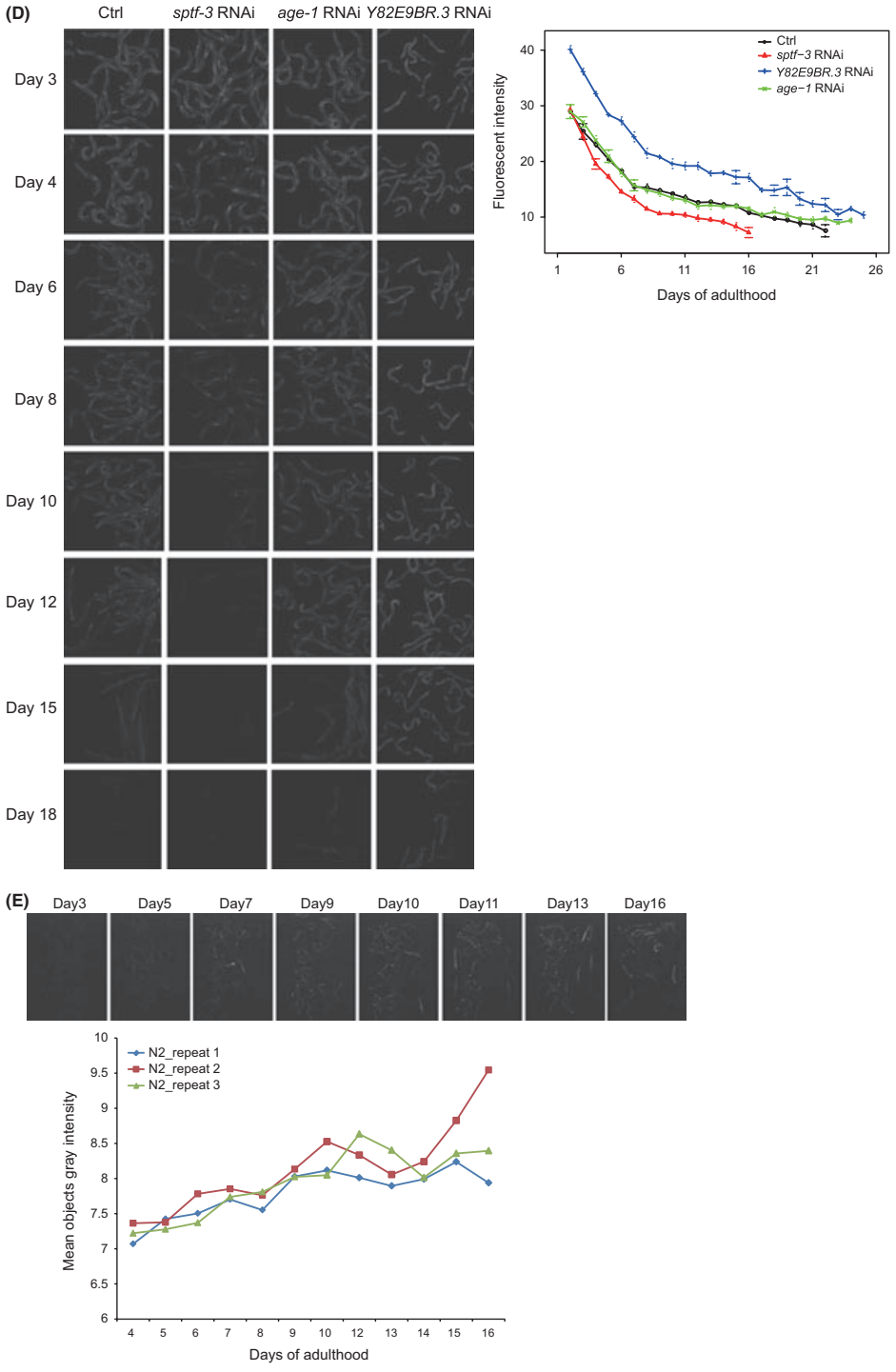

Fig. 4b (Continued).

MicroChem, Newton, MA, USA). The narrow sieve channels were fabricated by spin-coating negative photoresist (SU-8 2010, MicroChem) to a thickness of 10 μm. Other channels that can be controlled by the pneumatic valves were made of 80-μm-thick positive photoresist (AZ 50XT, AZ Electronic Materials). The patterned positive photoresist was re-flowed to obtain a rounded section. The 15-μm-thick mold of the control layer was made of positive photoresist (AZ P4620, AZ Electronic Materials, Branchburg, NJ, USA). The two master molds were treated with trimethylchlorosilane (Sinopharm, Shanghai, China) vapor for 5 min at room temperature before PDMS pouring. 30 g of uncured PDMS mixture (5:1, elastomer-to-cross-linker ratio) was poured onto the master

© 2013 John Wiley & Sons Ltd and the Anatomical Society

mold of fluid layer, degassed for 1 h, and then baked at 80 °C for 20 min. The control layer was fabricated by spin-coating uncured PDMS (20:1, elastomer-to-cross-linker ratio) onto the mold at 1200 rpm for 60 s and then was baked at 80 °C for 30 min. After the fluid layer was peeled off from its mold and hole-punched, it was aligned over the control layer and then baked at 80 °C for 45 min. The bonded 2-layer structure was then peeled off from the control mold, hole-punched, and placed on a thin, cured PDMS layer (10:1, elastomer-to-cross-linker ratio) covered glass slide. Finally, the whole chip was incubated at 80 °C for > 6 h to ensure the bonding between layers. We developed a Labview (National Instruments, Austin, TX, USA) program to control the valve actuation, and the fluid flow was driven by compressed air (0.1 MPa).

Worm Synchronization

Four dishes of gravid N2 hermaphrodites were washed off by M9 buffer and then collected and bleached by 5% solution of sodium hypochlorite. After washed by M9 buffer twice, the eggs were suspended in S-medium and allowed to hatch overnight in the absence of food, resulting in starved worms arrested in the L1 stage of development.

Lifespan assays

The day of egg-laying was defined as day 0 for all lifespan tests.

For RNAi-lifespan tests in WormFarm, synchronized L1 worms were distributed to RNAi plates, which had been spread with RNAi bacteria clones, and maintained at 20 °C till adulthood. When reaching adult day 2, worms were washed off the plate and loaded into PDMS chambers of the WormFarm chips and incubated at 25 °C. HT115 bacteria, with RNAi vectors containing different fragments of target genes, were induced by IPTG, suspended in the S-Medium, and passed through the chambers. Fungizone (250 ug L^{-1}) and Amp (100 mg L^{-1}) were added into the S-Medium to prevent the contamination. Bacteria culture was manually changed every day in the food container to maintain fresh food supply.

For the glucose lifespan test in WormFarm, the synchronized L1 worms were cultured on the NGM plates with OP50 bacteria at 20 °C till adulthood. Adult day 2 worms were washed off the plates, loaded into PDMS chambers, and incubated at 25 °C. Fresh live OP50 bacteria stored were suspended in the S-Medium containing different concentrations of glucose (0, 2 and 4%) and passed through the chambers. Fungizone (250 ug L^{-1}) were added into the S-Medium to prevent contamination. Bacteria culture was manually changed every day in the food container to maintain fresh food supply.

Photos and movies of each chamber were taken every 24 h using a CCD camera (DP72, Olympus, Japan) on a zoom stereomicroscope (SMZ1000, Nikon, Japan).

For parallel experiments on NGM agar plates, adult day 2 worms on the RNAi plates were transferred onto new RNAi plates containing 20 μg mL^{-1} FUdR and scored for survival rate every day. Adult day 2 worms for glucose test on NGM plates with OP50 were transferred onto new NGM plates containing 20 μg mL^{-1} FUdR and different concentrations of glucose (0, 2, and 4%) and scored for survival rate every day. Temperature setting was exactly the same as the lifespan test in WormFarm chip: worms grown up at 20 °C and spent adulthood at 25 °C. Worms were transferred to fresh plates every 4 days. Worms that crawled off the plates were excluded from the experiments. All experiments were independently performed at least twice.

Quantitation of the worm phenotypes

All images and videos were collected using a zoom stereomicroscope (Nikon SMZ1000) with a CCD camera (Olympus DP72). The field of view was set to cover one or two chambers for each shot.

To automatically quantitate the survival rate and other phenotypes including worm size, length, and width, we developed a new computational algorithm to analyze the images in three steps.

Step 1: Video preprocessing

We mark the chamber region by first identifying the reference circle in the center of the chip in each frame and then determine the boundaries based on the relative distance to the center of the reference. We then covert the gray-scale images to black and white (BW) images according to Otsu's method (Otsu, 1979). A closed object in the BW image is labeled as a worm-like object (WLO) if its size is $\geq$ 80 pixels.

Step 2: Obtain the maximum area of a single worm (A_{ms})

We define the maximum area in pixels of any single worm (A_{ms}) as 1.5-fold of the median of the WLO's areas on the first video when there is rarely any worm cluster. The A_{ms} is then used to identify single worm and to determine the number of worms in the worm clusters in subsequent videos of older adults, which often contain 2–10 worms per cluster and an average of 35% of the worms clustered in total.

Step 3: Quantitating worm phenotypes

To estimate the number of worms in each WLO, we first label an object as having moved since the last frame (object M) if the nonoverlapping area of the two overlapping WLOs between two frames is > 3% of the union of the two areas. Then, for each M, if its area is $\leq A_{ms}$, the object is labeled as a single worm (SM), and its area, circumference, length, width, mobility (moving area divided by total area) is calculated and recorded (Note S1). And the average size of SMs per chamber, per video is defined as A_{as}. If M's area is $> A_{ms}$, we count the number of single worms as the rounding of the area of M divided by A_{as}. Finally, we calculate the mean value of the worm area/length/width/mobility of all the frames in the video as the average quantified worm phenotypes at a time point (Note S1).

We describe the shape of a worm according to a published method (Stephens *et al.*, 2008). Each single worm was thinned to a backbone (a line of one pixel thick through the center of worm body). We then sliced the backbone to 60 segments to equal arc length and computed each segment's intersection angle with the horizontal axis. To make it independent of coordinate system, all the angles were standardized by subtracting the average of the angles.

© 2013 John Wiley & Sons Ltd and the Anatomical Society

A vector of 60 standardized angles of each worm defines the shape of the worm. The average absolute value in each vector was used for PCA. Other features are described in Note S1 (Supporting information), and Image Analysis Tutorials with snapshots are shown in Note S2 (Supporting information).

Mitochondria visualization

Mitochondria were visualized using *Pmyo-3::mito::GFP* construct (Labrousse *et al.*, 1999). We injected the *Pmyo-3::mito::GFP* plasmid into N2 and obtained the stable transgenic line by gamma irradiation.

Real-time *in vivo* fluorescent measurement

For fluorescent intensity of *Pmyo-3::mito::GFP*, N2 worms carrying the *Pmyo-3::mito::GFP* transgene were filmed every day using a fluorescence stereomicroscope with camera (Nikon SMZ1000, Olympus DP72 CCD). The exposure time was set as 50 ms, and sensitivity was ISO1600.

For intestinal auto-fluorescence, N2 worms were filmed every day. The exposure time was set as 200 ms, and sensitivity was ISO1600.

After converting the gray-scale fluorescence images to black and white, we calculated the average signal intensity per pixel per daily image (2× magnification).

For each frame in the fluorescence videos, the pixels that the gray-scale value < 5 were regarded as background, then we could get the objects (each closed area was regarded as an object except those whose area was < 6 pixel); for each objects, the average fluorescent intensity (F) was represented as the average gray-scale values for all the pixels (Note S1). Finally, the F for a video was represented as the average of the F values of the objects from all frames in the video.

Acknowledgments

We thank Bo Zheng (The Chinese University of Hong Kong) for the initial prototype design, Axel Mosig for discussions on image analysis, and Dangsheng Li and Christopher Green for critical reading of the manuscript. We thank CGC and Alexander M. van der Bliek for kindly sending us the *Pmyo-3::mito::GFP* constructs and worms. This work was supported by grants from the Chinese Ministry of Science and Technology (Grant #2011CB504206 and 2011CB809106), to J.D.J.H and Y.H., grants from the National Natural Science Foundation of China (Grant 31210103916, 91019019, 20890020, 90913011 and 21222501) to J.D.J.H and Y.H., and grants from Chinese Academy of Sciences (Grant #KSCX2-EW-R-02, KSCX2-EW-J-15, Y2201242 and XDA01010303) to J.D.J.H.

Author Contributions

JDJH conceived the project. YH, JDJH, JS, BX, and YP designed the fluidic device. JDJH, YH and BX, JS designed experiments. JDJH, WC, and NQ designed computational analyses. JS, BX, DJ, and YM implemented the fluidic device. BX, SJ, NS, and TY implemented the experiments. WC, NQ, and ZH implemented computational analysis. JDJH, BX, YH, JS, WC, NQ, and MK wrote the paper. JDJH and YH provided financial support.

References

Aitlhadj L, Sturzenbaum SR (2010) The use of FUdR can cause prolonged longevity in mutant nematodes. *Mech. Ageing Dev.* **131**, 364–365.

Bishop NA, Guarente L (2007) Two neurons mediate diet-restriction-induced longevity in *C. elegans*. *Nature* **447**, 545–549.

Brenner S (1974) The genetics of *Caenorhabditis elegans*. *Genetics* **77**, 71–94.

Davies SK, Leroi AM, Bundy JG (2012) Fluorodeoxyuridine affects the identification of metabolic responses to daf-2 status in *Caenorhabditis elegans*. *Mech. Ageing Dev.* **133**, 46–49.

Davis BO Jr, Anderson GL, Dusenbery DB (1982) Total luminescence spectroscopy of fluorescence changes during aging in *Caenorhabditis elegans*. *Biochemistry* **21**, 4089–4095.

Finkel T, Holbrook NJ (2000) Oxidants, oxidative stress and the biology of ageing. *Nature* **408**, 239–247.

Fraser AG, Kamath RS, Zipperlen P, Martinez-Campos M, Sohrmann M, Ahringer J (2000) Functional genomic analysis of *C. elegans* chromosome I by systematic RNA interference. *Nature* **408**, 325–330.

Gandhi S, Santelli J, Mitchell DH, Stiles JW, Sanadi DR (1980) A simple method for maintaining large, aging populations of *Caenorhabditis elegans*. *Mech. Ageing Dev.* **12**, 137–150.

Gerstbrein B, Stamatas G, Kollias N, Driscoll M (2005) In vivo spectrofluorimetry reveals endogenous biomarkers that report healthspan and dietary restriction in *Caenorhabditis elegans*. *Aging Cell* **4**, 127–137.

Greer EL, Maures TJ, Hauswirth AG, Green EM, Leeman DS, Maro GS, Han S, Banko MR, Gozani O, Brunet A (2010) Members of the H3K4 trimethylation complex regulate lifespan in a germline-dependent manner in *C. elegans*. *Nature* **466**, 383–387.

Huang C, Xiong C, Kornfeld K (2004) Measurements of age-related changes of physiological processes that predict lifespan of *Caenorhabditis elegans*. *Proc Natl Acad Sci U S A* **101**, 8084–8089.

Hulme SE, Shevkoplyas SS, McGuigan AP, Apfeld J, Fontana W, Whitesides GM (2010) Lifespan-on-a-chip: microfluidic chambers for performing lifelong observation of *C. elegans*. *Lab Chip* **10**, 589–597.

Joeng KS, Song EJ, Lee KJ, Lee J (2004) Long lifespan in worms with long telomeric DNA. *Nat. Genet.* **36**, 607–611.

Johnson TE (1990) Increased life-span of age-1 mutants in *Caenorhabditis elegans* and lower Gompertz rate of aging. *Science* **249**, 908–912.

Kenyon C (2005) The plasticity of aging: insights from long-lived mutants. *Cell* **120**, 449–460.

Kenyon CJ (2010) The genetics of ageing. *Nature* **464**, 504–512.

Klass MR (1977) Aging in the nematode *Caenorhabditis elegans*: major biological and environmental factors influencing life span. *Mech. Ageing Dev.* **6**, 413–429.

Labrousse AM, Zappaterra MD, Rube DA, van der Bliek AM (1999) *C. elegans* dynamin-related protein DRP-1 controls severing of the mitochondrial outer membrane. *Mol. Cell* **4**, 815–826.

Lee SS, Lee RY, Fraser AG, Kamath RS, Ahringer J, Ruvkun G (2003) A systematic RNAi screen identifies a critical role for mitochondria in *C. elegans* longevity. *Nat. Genet.* **33**, 40–48.

Lee SJ, Murphy CT, Kenyon C (2009) Glucose shortens the life span of *C. elegans* by downregulating DAF-16/FOXO activity and aquaporin gene expression. *Cell Metab.* **10**, 379–391.

Lee SS, Avalos Vizcarra I, Huberts DH, Lee LP, Heinemann M (2012) Whole lifespan microscopic observation of budding yeast aging through a microfluidic dissection platform. *Proc Natl Acad Sci U S A* **109**, 4916–4920.

Leiser SF, Begun A, Kaeberlein M (2011) HIF-1 modulates longevity and healthspan in a temperature-dependent manner. *Aging Cell* **10**, 318–326.

Lin K, Dorman JB, Rodan A, Kenyon C (1997) daf-16: an HNF-3/forkhead family member that can function to double the life-span of *Caenorhabditis elegans*. *Science* **278**, 1319–1322.

Martin GM, Austad SN, Johnson TE (1996) Genetic analysis of ageing: role of oxidative damage and environmental stresses. *Nat. Genet.* **13**, 25–34.

McCarroll SA, Murphy CT, Zou S, Pletcher SD, Chin CS, Jan YN, Kenyon C, Bargmann CI, Li H (2004) Comparing genomic expression patterns across species identifies shared transcriptional profile in aging. *Nat. Genet.* **36**, 197–204.

© 2013 John Wiley & Sons Ltd and the Anatomical Society

Mitchell DH, Stiles JW, Santelli J, Sanadi DR (1979) Synchronous growth and aging of *Caenorhabditis elegans* in the presence of fluorodeoxyuridine. *J Gerontol.* **34**, 28–36.

Morris JZ, Tissenbaum HA, Ruvkun G (1996) A phosphatidylinositol-3-OH kinase family member regulating longevity and diapause in *Caenorhabditis elegans*. *Nature* **382**, 536–539.

Ogg S, Paradis S, Gottlieb S, Patterson GI, Lee L, Tissenbaum HA, Ruvkun G (1997) The Fork head transcription factor DAF-16 transduces insulin-like metabolic and longevity signals in *C. elegans*. *Nature* **389**, 994–999.

Otsu N (1979). A threshold selection method from gray-level histograms. *IEEE Trans. Systems Man and Cybernet* **9**, 62–66.

Pincus Z, Slack FJ (2010) Developmental biomarkers of aging in *Caenorhabditis elegans*. *Dev. Dyn.* **239**, 1306–1314.

Pincus Z, Smith-Vikos T, Slack FJ (2011) MicroRNA predictors of longevity in *Caenorhabditis elegans*. *PLoS Genet.* **7**, e1002306.

Schlotterer A, Kukudov G, Bozorgmehr F, Hutter H, Du X, Oikonomou D, Ibrahim Y, Pfisterer F, Rabbani N, Thornalley P, Sayed A, Fleming T, Humpert P, Schwenger V, Zeier M, Hamann A, Stern D, Brownlee M, Bierhaus A, Nawroth P, Morcos M (2009) *C. elegans* as model for the study of high glucose- mediated life span reduction. *Diabetes* **58**, 2450–2456.

Schulz TJ, Zarse K, Voigt A, Urban N, Birringer M, Ristow M (2007) Glucose restriction extends *Caenorhabditis elegans* life span by inducing mitochondrial respiration and increasing oxidative stress. *Cell Metab.* **6**, 280–293.

Stephens GJ, Johnson-Kerner B, Bialek W, Ryu WS (2008) Dimensionality and dynamics in the behavior of *C. elegans*. *PLoS Comput. Biol.* **4**, e1000028.

Sutphin GL, Kaeberlein M (2009). Measuring *Caenorhabditis elegans* life span on solid media. *J. Vis Exp.* **27**, 1152.

Thorsen T, Maerkl SJ, Quake SR (2002) Microfluidic large-scale integration. *Science* **298**, 580–584.

Timmons L, Court DL, Fire A (2001) Ingestion of bacterially expressed dsRNAs can produce specific and potent genetic interference in *Caenorhabditis elegans*. *Gene* **263**, 103–112.

Unger MA, Chou HP, Thorsen T, Scherer A, Quake SR (2000) Monolithic microfabricated valves and pumps by multilayer soft lithography. *Science* **288**, 113–116.

Wahlby C, Kamentsky L, Liu ZH, Riklin-Raviv T, Conery AL, O'Rourke EJ, Sokolnicki KL, Visvikis O, Ljosa V, Irazoqui JE, Golland P, Ruvkun G, Ausubel FM, Carpenter AE (2012). An image analysis toolbox for high-throughput *C. elegans* assays. *Nat. Methods* **9**, 714–716.

Wang J, Zhou Y, Qiu H, Huang H, Sun C, Xi J, Huang Y (2009) A chip-to-chip nanoliter microfluidic dispenser. *Lab Chip* **9**, 1831–1835.

Xie Z, Zhang Y, Zou K, Brandman O, Luo C, Ouyang Q, Li H (2012). Molecular phenotyping of aging in single yeast cells using a novel microfluidic device. *Aging Cell* **11**, 599–606.

Xue H, Xian B, Dong D, Xia K, Zhu S, Zhang Z, Hou L, Zhang Q, Zhang Y, Han JD (2007) A modular network model of aging. *Mol Syst Biol.* **3**, 147.

Zahn JM, Poosala S, Owen AB, Ingram DK, Lustig A, Carter A, Weeraratna AT, Taub DD, Gorospe M, Mazan-Mamczarz K, Lakatta EG, Boheler KR, Xu X, Mattson MP, Falco G, Ko MS, Schlessinger D, Firman J, Kummerfeld SK, Wood WH 3rd, Zonderman AB, Kim SK, Becker KG (2007) AGEMAP: a gene expression database for aging in mice. *PLoS Genet.* **3**, e201.

Supporting Information

Additional Supporting Information may be found in the online version of this article at the publisher's web-site.

Fig. S1 The process of loading young adult worms into PDMS chamber.

Fig. S2 Worms living in PDMS chambers have a similar physiological growth as worms living on NGM plates.

Fig. S3 The reproducibility of worm lifespan assays upon RNAi of aging-related genes.

Fig. S4 The reproducibility of worm lifespan assays in glucose medium.

Fig. S5 Age-related changes in fluorescence intensities.

Fig. S6 Oxidative stress tolerance assay in WormFarm.

Fig. S7 Comparison of survival rates calculated from our computer program with or without considering clustered worms to those from manual counting.

Video S1 Load 2% pluronic solution to make the channel lubricant.

Video S2 Load young adult worms into PDMS chamber.

Video S3 Wash off the offspring of adult worms in PDMS chamber.

Video S4 Movie of 5-day old worms in PDMS chamber (upper panel, *sptf-3* RNAi; lower panel, Ctrl RNAi).

Video S5 Movie of 5-day old worms in PDMS chamber (upper panel, *age-1* RNAi; lower panel, *Y82E9BR.3* RNAi).

Note S1 Formulas for calculating worm features/phenotypes.

Note S2 WormFarm video analysis procedure.

Table S1 Log-rank test results between automatically counted mean lifespans of different repeats in RNAi experiments.

Table S2 Log-rank test results between automatically counted mean lifespans of different repeats of glucose die*t* test.

Table S3 Significances of difference between the RNAi groups for worm length, width, area and motility as determined by Student's *t*-test.

Table S4 Raw data for lifespan assays.

Table S5 Raw data for mitochondrial fluorescent density assay.

Table S6 Raw data of average values of worm phenotypic features used in principal component analysis.

© 2013 John Wiley & Sons Ltd and the Anatomical Society